

Supplementary information

Inhibition of oscillatory motion of a camphor float due to dissolution

Masakazu Kuze^{a, b}, Mai Tateishi^a, Yoshikatsu Hayashi^c, Muneyuki Matsuo^{a, d, *}, Satoshi Nakata^{a, *}

^a *Graduate School of Science, Hiroshima University, 1-3-1 Kagamiyama, Higashi-Hiroshima, Hiroshima 739-8526, Japan*

^b *Meiji Institute for Advanced Study of Mathematical Sciences (MIMS), Meiji University, 4-21-1 Nakano, Nakano-ku, Tokyo 164-8525, Japan*

^c *Department of Biomedical Sciences and Biomedical Engineering, School of Biological Sciences, University of Reading, Reading, Berkshire RG6 7BE, UK*

^d *Graduate School of Arts and Sciences, The University of Tokyo, 3-8-1 Komaba, Meguro, Tokyo 153-8902, Japan*

*To whom correspondence should be addressed.

E-mail: nakatas@hiroshima-u.ac.jp (SN), muneyuki@hiroshima-u.ac.jp (MM)

1. Movies of self-propulsion of a camphor float in Fig. 1

Movie S1. The movie on oscillatory motion at $[\text{Na}_2\text{SO}_4] = 0 \text{ M}$ in Fig. 1a ($\times 30$ speed)

Movie S2. The movie on oscillatory motion at $[\text{Na}_2\text{SO}_4] = 1.0 \text{ M}$ in Fig. 1b ($\times 30$ speed)

Movie S3. The movie on oscillatory motion at $[\text{Na}_2\text{SO}_4] = 1.7 \text{ M}$ in Fig. 1c ($\times 30$ speed)

2. The speed and motile length of the individual pulse-like motion

Fig. S1 shows the time-dependent profile of the speed change and trajectory of the single pulse-like motion at $C_i =$ (a) 0, (b) 1.0, and (c) 1.7 M, which correspond to those in Fig. 1 in the main text. The maximum speed and motile length decreased with an increase in C_i when the camphor float was accelerated.

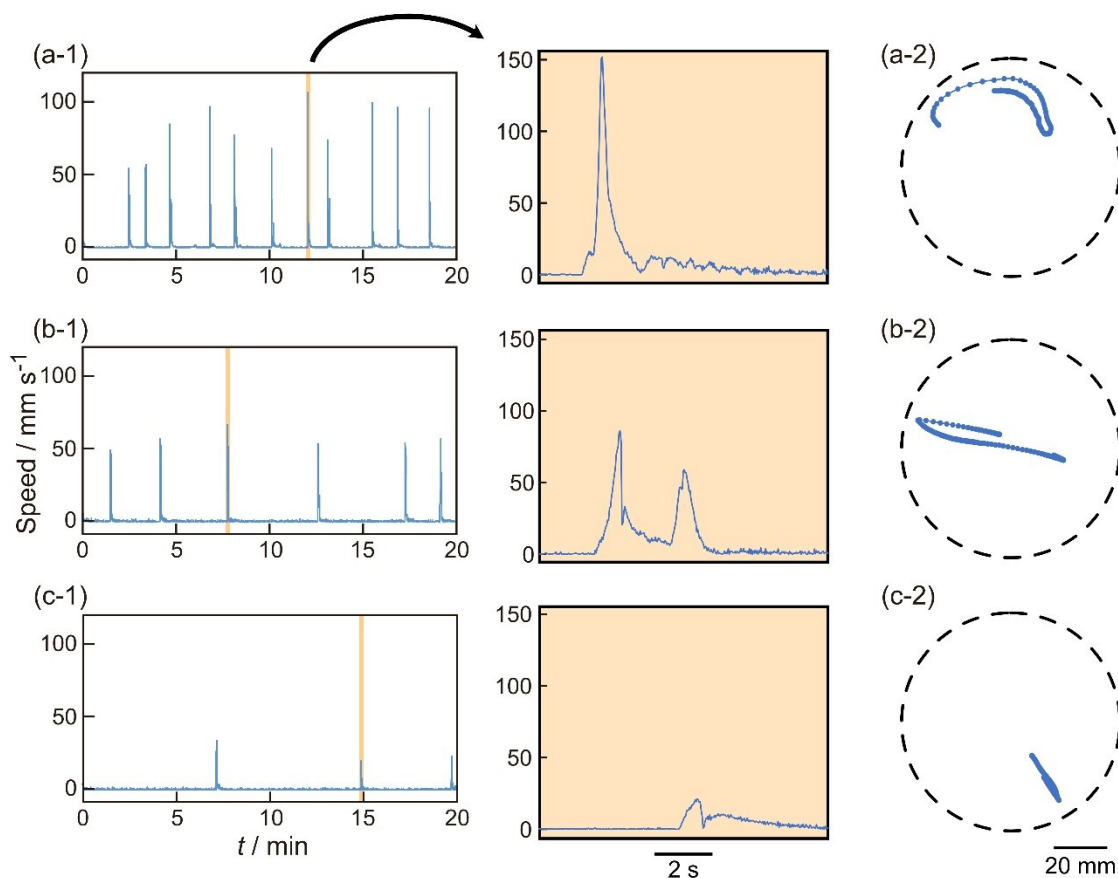


Fig. S1. Oscillatory motion of camphor float with variation of Na_2SO_4 concentration, $C_i =$ (a) 0, (b) 1.0, and (c) 1.7 M. (1) Time-variation of the speed of motion for camphor float. The right figures were obtained by enlarging the orange region (10 seconds) in the left images. (2) Trajectories on the center position of camphor float on the surface of aqueous phase (top-view) for 10 seconds. The time interval of motion was $1/30$ s. The dotted circles in (2) correspond to the boundary of the Petri dish.

3. Time variation of the mass of camphor dissolved in the Na_2SO_4 aqueous solution

We investigated the amount of camphor dissolved in the Na_2SO_4 aqueous solution as a function of time. As for the measurement of the dissolution of camphor into the Na_2SO_4 aqueous solution, six camphor disks (mass of a disk: 5 mg) were floated on a Na_2SO_4 aqueous solution (concentration of Na_2SO_4 : 0–1.7 M, volume: 24 mL) which was poured into the glass Petri dish (inner diameter: 70 mm, height: 20 mm). Then, the mass of the camphor disks was measured for every 2 mins after removing water from the disk. The concentration of camphor, C , was calculated with the value of the decrease

in the mass of the camphor disk and the volume of the aqueous phase (volume: 24 mL). Fig. S1 shows the time-variation on C . C linearly increased with time. This result suggests that the camphor molecules were difficult to dissolve to the aqueous solution at the higher concentration of Na_2SO_4 .

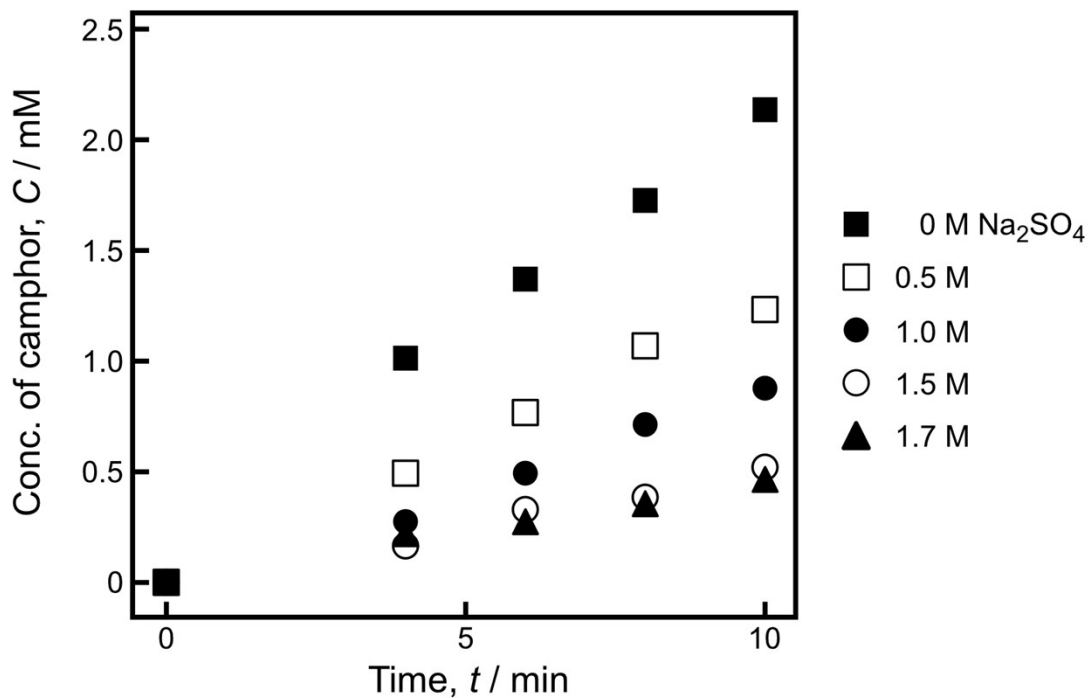


Fig. S2. The time-variation on the camphor concentration dissolved in the Na_2SO_4 aqueous solution.

3. The saturated concentration of camphor in the solution depending on concentration of Na_2SO_4 solution C_i

We measured the saturated concentration of camphor C_0 in the pure water and Na_2SO_4 solution. The solution was prepared by adding an excess amount of camphor under stirring at room temperature ($25 \pm 2^\circ\text{C}$) for 24 h. We took absorbance with a spectrophotometer (wavelength: 285 nm, UV-1650PC, Shimadzu, Kyoto, Japan). A calibration curve for camphor was prepared based on the absorbance at 285 nm in aqueous solutions of known concentrations. The saturated concentration of camphor was estimated according to the calibration curve. Fig. S3 shows C_0 depending on C_i . C_0 was decreased with an increase in C_i .

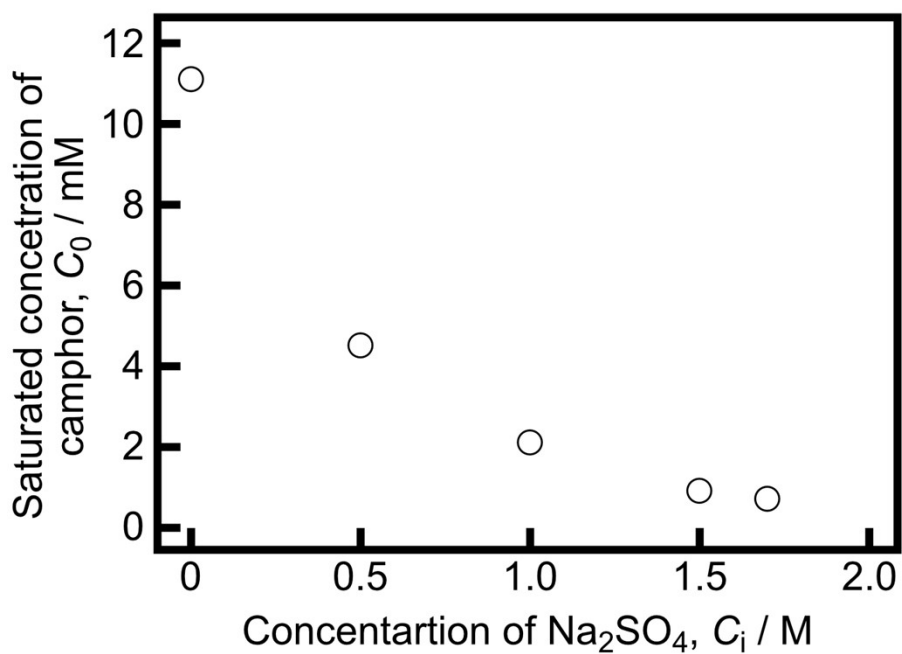


Fig. S3. The saturated concentration of camphor C_0 depending on C_i .

4. Relationship between frequency and kC_0

Fig. S4 shows frequency of oscillatory motion as a function of kC_0 . The frequency of oscillatory motion was proportional to kC_0 .

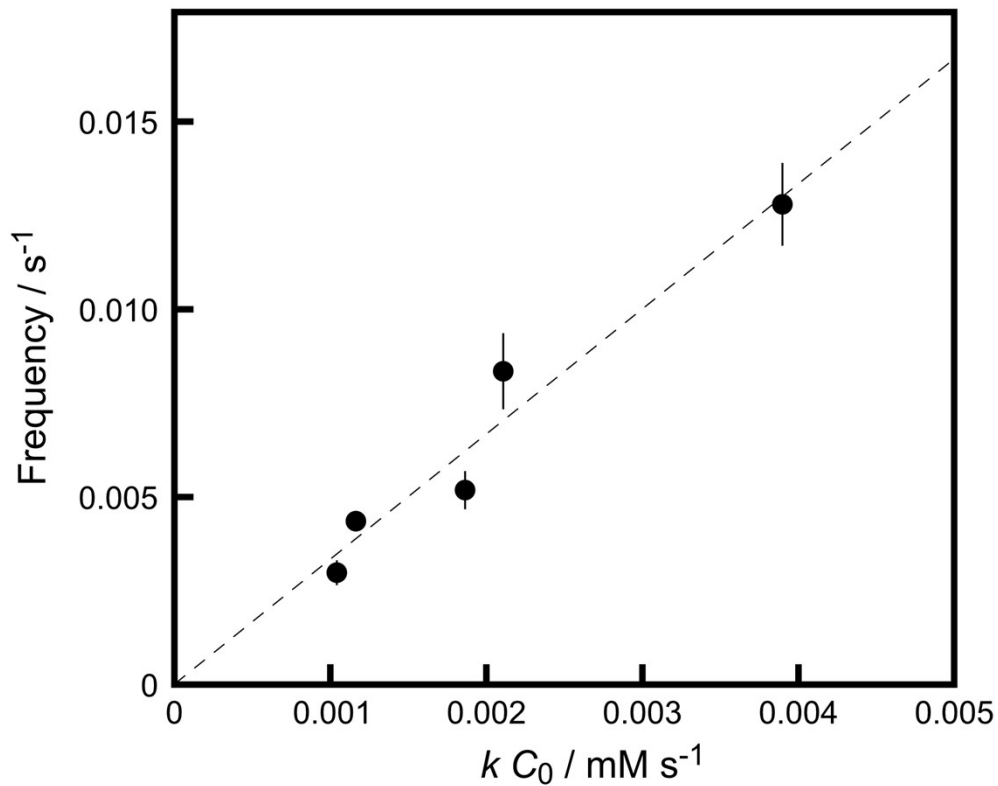


Fig. S4. The frequency of oscillatory motion for the camphor floats placed on Na_2SO_4 aqueous solutions depending on kC_0 . Error bars represent the standard deviation.